

ANALYSIS OF A MASS-SPRING-DAMPER SYSTEM'S RESPONSE UNDER STOCHASTIC LOADING: A WASSERSTEIN METRIC-BASED APPROACH

João Felipe Costa Lobato, Roberta Lima and Rubens Sampaio

Pontifícia Universidade Católica do Rio de Janeiro, Laboratório de Dinâmica e Vibrações. Rua Marquês de São Vicente, 225, Gávea, Rio de Janeiro, Brasil.

Keywords: Stationary Stochastic Processes, Random Vibrations, Engineer Metric, Wasserstein Metric.

Abstract. This paper investigates the response of a deterministic, linear, time-invariant mass-spring-damper system subjected to loading modelled as a stationary stochastic process. The primary objective is to determine, through numerical simulations using the Monte Carlo method, whether or not the system's response converges to a stationary stochastic process. The analysis employs two metrics: Engineer distance, which focuses on the proximity of distribution means, and Wasserstein distance, which provides a more robust comparison by quantifying divergence between probability distributions across different sections of the stochastic process. The methodology developed can be adapted for the analysis of other mechanical systems, including non-linear systems.

1 INTRODUCTION

This work aims to analyse the response of a deterministic, linear, and time-invariant system with one degree of freedom of the mass-spring-damper type, illustrated in Fig. 1, subjected to a load modelled as a stationary stochastic process.

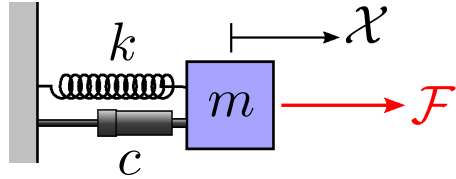


Figure 1: Analysed mass-spring-damper system.

The system parameters are: mass $m = 1$ kg, damping coefficient $c = 0.1$ Ns/m, and spring stiffness $k = 1$ N/m. The mass position is denoted by X , and zero initial conditions are assumed for both displacement and velocity. The amplitude F_a and frequency F_ω of the stochastic forcing \mathcal{F} are modelled as independent random variables, both normally distributed as $\mathcal{N}(1, 1/3)$. The system's governing equation is:

$$\ddot{X}(t) + 0.1\dot{X}(t) + X(t) = F_a \cos(F_\omega t). \quad (1)$$

Since the excitation \mathcal{F} is random, the system response X is also modelled as a stochastic process. The aim is to investigate whether the system response exhibits stationarity properties in the steady state (Lobato, 2024; Benaroya and Han, 2005).

Let T be an analysis interval, a stochastic process X is a function such that $\forall t \in T$, there exists a random variable $X(t)$ defined on a probability space $(\Omega, \mathcal{F}, \Pr)$.

Let T be a time interval. A stochastic process X is a function such that for all $t \in T$, there exists a random variable $X(t)$ defined on a probability space $(\Omega, \mathcal{F}, \Pr)$. A process is said to be strictly stationary if for any $m \in \mathbb{N}$ and any tuple $(t_1, \dots, t_m) \in T^m$, the joint distribution of $(X(t_1), \dots, X(t_m))$ is identical to that of $(X(t_1 + \Delta t), \dots, X(t_m + \Delta t))$ for all $\Delta t \in \mathbb{R}$. It is said to be weakly stationary if this equality occurs only for $m = 1$ and $m = 2$.

The goal of this study is to verify whether the system response exhibits steady-state stationarity according to the aforementioned definitions. The analysis is carried out through numerical simulations using the Monte Carlo method (Sampaio and Lima, 2012), in which multiple realizations of the excitation are generated, and for each realization, the system response is computed via an algebraic expression (Inman, 2014) over a specified time interval.

From the resulting response realizations, a statistical model of the system response is constructed by computing sample means over time and normalized histograms for different sections of the stochastic process. The number of realizations is determined through a convergence analysis: the number is increased until the computed statistics stabilize within a predefined tolerance. Because the Monte Carlo method does not yield joint probability distributions for $(X(t_1), \dots, X(t_m))$, but rather normalized histograms, two main challenges arise. The first is that comparing histograms is generally limited to visual inspection, which is imprecise. The second is that visualizing histograms is restricted to $m = 1$ and $m = 2$, i.e., at most, the joint histogram of two sections of the stochastic process can be observed.

In order to overcome the limitations of visual histogram comparisons and the restriction on visualizing bivariate histograms, metrics will be used to compare the joint probability distributions of up to five sections of the stochastic process that describes the system response. Two

metrics will be employed: the Engineer distance and the Wasserstein distance, as described in Section 2.

2 ENGINEER AND WASSERSTEIN METRICS

Let $X = \mathcal{X}(t_1)$ and $Y = \mathcal{X}(t_2)$ be two random variables originating from a stochastic process \mathcal{X} . Their probability distributions are p_X and p_Y respectively. The Engineer distance between them is given by Eq. (2) (Rachev et al., 2013):

$$\mathcal{E}(p_X, p_Y) = |\mathbb{E}[X] - \mathbb{E}[Y]| = \left| \int_{\mathbb{R}} x(p_X(x) - p_Y(x))dx \right|, \quad (2)$$

if X and Y have means. When the probability densities of X and Y are unknown, but one has n realizations of these random variables, given by $x^{(1)}, \dots, x^{(n)}$ and $y^{(1)}, \dots, y^{(n)}$, it is possible to calculate an approximation for the Engineer distance \mathcal{X}_1 and \mathcal{X}_2 by Eq. (3):

$$\hat{\mathcal{E}}(p_X, p_Y) = \left| \frac{1}{n} \sum_{i=1}^n x^{(i)} - \frac{1}{n} \sum_{i=1}^n y^{(i)} \right|. \quad (3)$$

Let $X = \mathcal{X}(t_1)$ and $Y = \mathcal{X}(t_2)$ be two continuous random variables with probability densities p_X and p_Y and cumulative probability distributions P_X and P_Y respectively. The Wasserstein distance of order q \mathcal{W}_q between them is given by Eq (4) (Deza and Deza, 2016):

$$\mathcal{W}_q(p_X, p_Y) = (\inf \mathbb{E}[|X - Y|^q])^{1/q} = \left(\int_{\mathbb{R}} |P_X(x) - P_Y(x)|^q dx \right)^{1/q}. \quad (4)$$

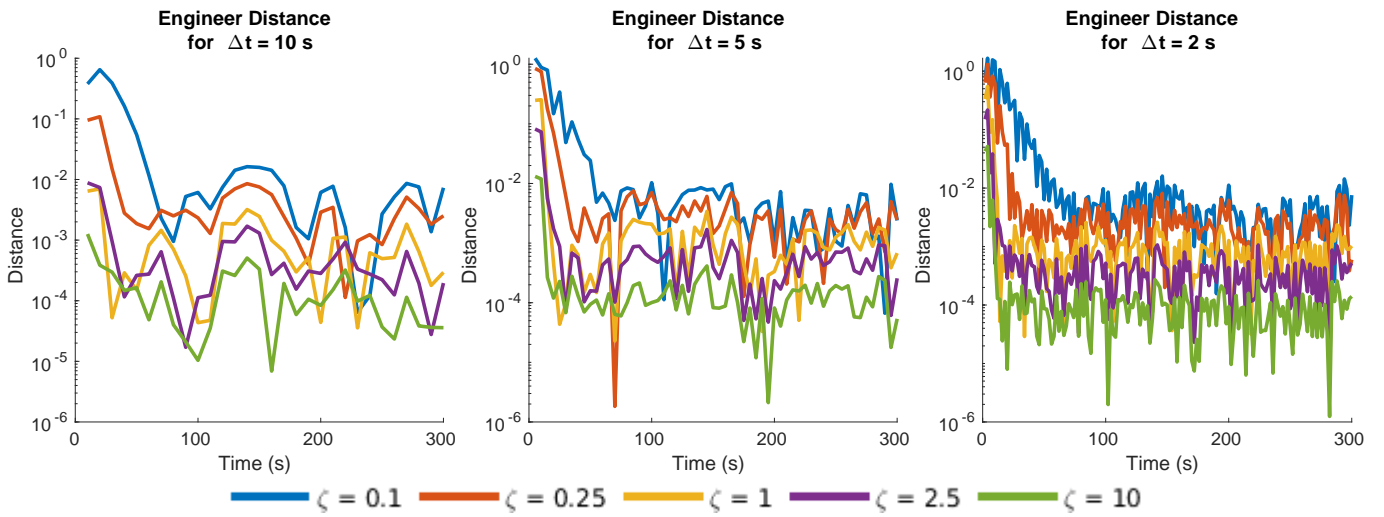
Similarly to the Engineer distance, it is possible to compute an approximation to the Wasserstein distance when the probability densities of \mathcal{X}_1 and \mathcal{X}_2 are unknown, but there are realizations of these random variables. Let $x_1^{(1)}, \dots, x_1^{(n)}$ and $x_2^{(1)}, \dots, x_2^{(n)}$ be realizations of \mathcal{X}_1 and \mathcal{X}_2 ordered in increasing order such that $x_1^{(1)} \leq \dots \leq x_1^{(n)}$ and $x_2^{(1)} \leq \dots \leq x_2^{(n)}$. An approximation for the Wasserstein distance X and Y can be calculated by the equation (5):

$$\hat{\mathcal{W}}_q(p_X, p_Y) = \left(\frac{1}{n} \sum_{i=1}^n |x^{(i)} - y^{(i)}|^q \right)^{1/q}. \quad (5)$$

The Wasserstein distance can also be defined for random vectors with dimension $m > 1$. Let $\mathbf{X} = [\mathcal{X}(t_1), \mathcal{X}(t_2), \dots, \mathcal{X}(t_m)]^\top$ and $\mathbf{Y} = [\mathcal{X}(t_{m+1}), \dots, \mathcal{X}(t_{2m})]^\top$ be two random vectors in \mathbb{R}^m containing different sections of the stochastic process \mathcal{X} and probability distributions $p_{\mathbf{X}}$ and $p_{\mathbf{Y}}$ respectively. The Wasserstein distance between $p_{\mathbf{X}}$ and $p_{\mathbf{Y}}$ is given by Eq. (6) (Bigot, 2020):

$$\mathcal{W}_{q,m}(p_{\mathbf{X}}, p_{\mathbf{Y}}) = \inf_{\pi \in \Gamma(p_{\mathbf{X}}, p_{\mathbf{Y}})} \left(\int_{\mathbb{R}^m} |\mathbf{x} - \mathbf{y}|^q d\pi(\mathbf{x}, \mathbf{y}) \right)^{1/q}, \quad (6)$$

where $\Gamma(p_{\mathbf{X}}, p_{\mathbf{Y}})$ is the set of probability measures (also called transport plans) in $\mathbb{R}^m \times \mathbb{R}^m$ with respective marginal distributions $p_{\mathbf{X}}$ and $p_{\mathbf{Y}}$.

Figure 2: Engineer distances for different Δt and damping factors.

3 NUMERICAL SIMULATION RESULTS

3.1 Engineer Distances: Influence of the Damping Factor

Figure 2 presents the approximations for the Engineer distances between the sections $\mathcal{X}(t)$ and $\mathcal{X}(t + \Delta t)$, calculated for different values of the damping ratio $\zeta = \frac{c}{2\sqrt{mk}}$, considering fixed intervals of Δt . The horizontal axis represents the time t (in seconds), while the vertical axis, in logarithmic scale, shows the values of the Engineer distances. It is important to highlight that, for each point in the graph, the position on the t axis indicates the starting instant of the section $\mathcal{X}(t)$, while $\mathcal{X}(t + \Delta t)$ is defined based on the fixed Δt .

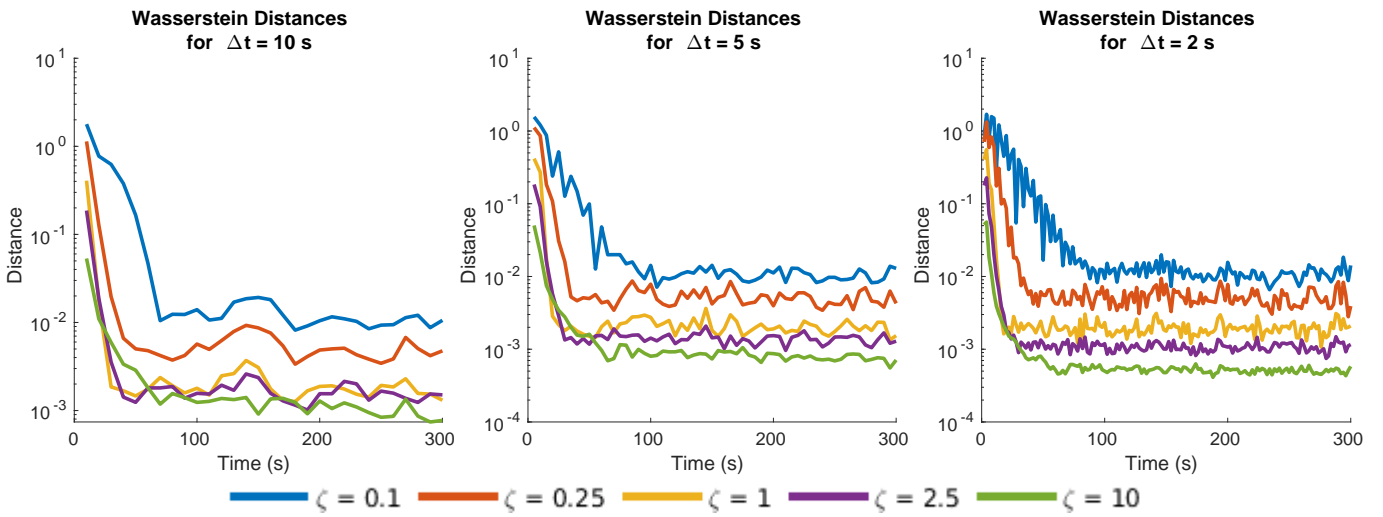
Each curve in the graph corresponds to a specific value of ζ , which allows us to observe how damping affects distance approximations over time. The behaviour of the curves shows that higher damping values result in faster convergence of distances to values close to zero, indicating less variation between the distributions of the compared sections. However, the stabilization of the sample Engineer distances is not sufficient to assert that the system response converges to a stationary stochastic process, since stationariness requires that the joint probability distributions of the process sections remain invariant over time, not just the stability of the first-order moments.

3.2 Wasserstein distances

Applying the Eq. (5), the Wasserstein distances between the position distributions were calculated for different intervals, changing certain parameters. The default dimension and order are $m = 1$ and $q = 2$ respectively.

3.2.1 Influence of the Damping Factor

Similarly to what was done for the Engineer distance, an analysis was made of the influence of the damping factor ζ of the system on the approximations for the Wasserstein distances between the sections $\mathcal{X}(t)$ and $\mathcal{X}(t + \Delta t)$. Through the results obtained, shown in Figure 3, it can be seen that the greater the damping, the faster the Wasserstein distances decay, indicating less variation between the distributions of the compared sections.

Figure 3: Wasserstein distances for different Δt and damping factors ζ for $q = 2$.

3.2.2 Influence of the Dimension

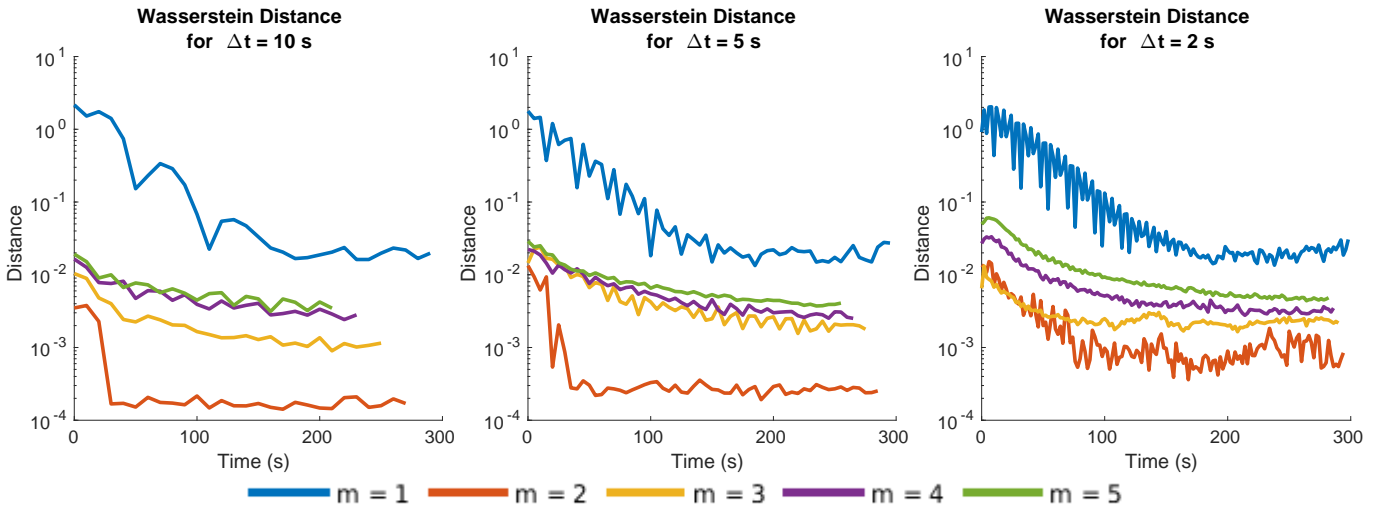
Figure 4: Wasserstein distances for different Δt and dimensions m for $q = 2$.

Figure 4 shows the computed approximations of the Wasserstein distances between the probability distributions of the random vectors \mathbf{X} and $\mathbf{Y} \in \mathbb{R}^m$. These vectors represent joint distributions of up to five sections, with $m \in \{1, 2, 3, 4, 5\}$, corresponding to the response \mathcal{X} for different values of Δt . For each value of Δt , the sections are uniformly selected with a spacing of Δt , resulting in the following definitions: $\mathbf{X} = [\mathcal{X}(t_1), \mathcal{X}(t_2), \dots, \mathcal{X}(t_m)]^\top$ and $\mathbf{Y} = [\mathcal{X}(t_{m+1}), \dots, \mathcal{X}(t_{2m})]^\top$, with the condition that $t_j = t_1 + (j-1)\Delta t$ for $j = 1, \dots, 2m$. For each point in the graph, the position on the time axis indicates the initial instant selected for the section $\mathcal{X}(t_1)$. It is observed that the distances converge for all dimensions, with the slowest convergence occurring for $m = 1$.

4 CONCLUSIONS

This paper investigated the response of a deterministic mass-spring-damper system subjected to a loading described by a stationary stochastic process. The main objective was to use numer-

ical approximations of the engineering and Wasserstein distances to assess whether or not the system's response would exhibit characteristics of stationarity in the steady-state regime. The Engineer distance, focused on the proximity of distribution means, was useful for a preliminary assessment, while the Wasserstein distance provided a more robust comparison, allowing for the quantification of divergence between the approximated probability distributions at different sections of the stochastic process.

Furthermore, due to the use of the Monte Carlo method, the joint probability distribution of different sections of the system response was unknown, with only histograms available. This created challenges for comparisons, since comparing histograms is, in principle, an imprecise task requiring visual inspection. Furthermore, histogram visualization is limited to a maximum of two sections of the stochastic process simultaneously. In this context, the use of the Wasserstein distance proved crucial to overcoming these limitations. This metric was used to compare the joint probability distributions of up to five sections of the stochastic process.

Finally, the methodology developed in this study can be adapted for the analysis of other mechanical systems, including non-linear systems. Its usefulness lies in the lack of general theoretical results for characterizing stationarity in systems of this type.

REFERENCES

- Benaroya H. and Han S. *Probability Models in Engineering and Science*. Taylor & Francis Group, LLC, Boca Raton FL, United States, 2005. ISBN 978-0-8247-2315-6.
- Bigot J. Statistical data analysis in the wasserstein space. *ESAIM: Proceedings and Surveys*, 68:1–19, 2020. <http://doi.org/10.1051/proc/202068001>.
- Deza M.M. and Deza E. *Encyclopedia of Distances*. Springer, Russia, France, 4 edition, 2016. ISBN 978-3-662-52844-0. <http://doi.org/10.1007/978-3-662-52844-0>.
- Inman D.J. *Engineering vibrations*. Pearson Education, New Jersey, United States, 4 edition, 2014. ISBN 978-0-13-287169-3.
- Lobato J.F.C. *Desenvolvimento de uma metodologia para análises estatísticas de um sistema massa-mola-amortecedor excitado por um carregamento estocástico*, 2024. <http://doi.org/10.17771/PUCRio.acad.68856>. Graduation Project, Department of Mechanical Engineering, PUC-Rio, Rio de Janeiro.
- Rachev S.T., Klebanov L.B., Stoyanov S.V., and Fabozzi F.J. *The Methods of Distances in the Theory of Probability and Statistics*. Springer, United States, Czechia, Singapore, France, 2013. ISBN 978-1-4614-4869-3. <http://doi.org/10.1007/978-1-4614-4869-3>.
- Sampaio R. and Lima R. *Modelagem estocástica e geração de amostras de variáveis e vetores aleatórios*, volume 70 of *Notas em Matemática Aplicada*. Sociedade Brasileira de Matemática Aplicada e Computacional, São Carlos - SP, Brazil, 2012.